

# We are IntechOpen, the world's leading publisher of Open Access books Built by scientists, for scientists

6,900

Open access books available

186,000

International authors and editors

200M

Downloads

Our authors are among the

154

Countries delivered to

TOP 1%

most cited scientists

12.2%

Contributors from top 500 universities



WEB OF SCIENCE™

Selection of our books indexed in the Book Citation Index  
in Web of Science™ Core Collection (BKCI)

Interested in publishing with us?  
Contact [book.department@intechopen.com](mailto:book.department@intechopen.com)

Numbers displayed above are based on latest data collected.  
For more information visit [www.intechopen.com](http://www.intechopen.com)



# Elaboration and Characterization of Calcium Phosphate Biomaterial for Biomedical Applications

Foued Ben Ayed

*Laboratory of Industrial Chemistry, National School of Engineering, Box 1173, 3038 Sfax  
Tunisia*

## 1. Introduction

Calcium phosphates constitute an important family of biomaterials resembling the part of calcified tissues. This study is based on calcium phosphate such as hydroxyapatite ( $\text{Ca}_{10}(\text{PO}_4)_6(\text{OH})_2$ , Hap), fluorapatite ( $\text{Ca}_{10}(\text{PO}_4)_6\text{F}_2$ , Fap) and tricalcium phosphate ( $\text{Ca}_3(\text{PO}_4)_2$ , TCP) phases because their chemical composition is similar to that of bone mineral (Hench, 1991; Legeros, 1993; Uwe et al., 1993; Elliott, 1994; Landi et al., 2000; Varma et al., 2001; Destainville et al., 2003; Wang et al., 2004; Ben Ayed et al., 2000, 2001a, b; 2006a, b; 2007; 2008a, b; Bouslama et al., 2009; Chaari et al., 2009). The most frequent is  $\beta$ -TCP because it is resorbable and osteoinductive (Gaasbeek et al., 2005; Steffen et al., 2001).  $\beta$ -TCP is resorbed in vivo by osteoclasts and replaced by new bone (Schilling et al., 2004). The tricalcium phosphate has been used clinically to repair bone defects for many years. However, mechanical properties of calcium phosphates are generally inadequate for many load-carrying applications. The tricalcium phosphate has a low density decreasing the mechanical properties. But, the efficiency of bi-phasic calcium phosphate (BCP) has been fully importantly efficiency its clinical efficacy to combat the chronic osteomyelitis in the long term. To our knowledge, if it is possible to vary the composition of bioceramic materials (composed of Hap and  $\beta$ -TCP) with its inherent porosity, it could be a solution owing to the faster resorption of this BCP together with the sustained release of the antibiotic.

In the literature Hap,  $\beta$ -TCP or the combination of both (Hap/TCP) was the most commonly used synthetic augments in high tibial osteotomy (Haell et al., 2005; Koshino et al., 2003; Gaasbeek et al., 2005; Van Hemert et al., 2004; Gutierrez et al., 2007). The use of bone cement as a temporary spacer for bone defects has been described, but secondary biological reconstruction was performed after cement removal (DeSilva et al., 2007). However, permanent acrylic bone cement has been used as an interface in the postero-medial part of high tibial osteotomy to maintain the opening angle and good results have been achieved (Hernigou et al., 2001). However, due to the different biomechanical features between bone and bone cement and missing bony remodelling and incorporation, the use of bone cement as a permanent spacer was not recommended, if one aims to achieve biological regeneration. Recently, Jensen and colleagues described that rapid resorption of  $\beta$ -TCP might impair the regenerative ability of local bone, especially in the initial stage of bone healing (Jensen et al.,

2006). The microstructure of the used  $\beta$ -TCP has important influence on the osteogenic effects (Okuda et al., 2007). This has recently been confirmed by Fellah and colleagues (Fellah et al., 2008). They show that the Hap/TCP with different micropores was evaluated in a goat critical-defect model.

Several research studies dealt with the question where and how to perform the osteotomy and which fixation material is most beneficial (Brouwer et al., 2006; Agneskirchner et al., 2006). Aryee et al. demonstrate histologically and radiologically that the complete rebuilding of lamelliform bone in patients without synthetic augmentation, whilst bony in growth into the Hap/TCP wedge of augmented osteotomies just slowly progressed (Aryee et al., 2008). In contrast to diminished osteotomies, there was no advantage in using Hap/TCP wedges or the combination of Hap/TCP wedges and platelet rich plasma (PRP) as supporting material after 12 months. In cases where augmentation is performed, either autologous spongy iliac bone graft or an Hap/TCP wedge of appropriate size was inserted into the osteotomy opening and pushed laterally until it is firmly aligned to the tibial bone. The Hap/TCP wedge utilised by us consists of 60% micro-macroporous biphasic Hap and 40%  $\beta$ -TCP. The average total porosity is 65–75%, whilst two different sizes of porosity are found within this material. The microporous part consists of pores with a diameter less than 10 $\mu$ m. The macroporous part consists of pores with a diameter between 300 $\mu$ m and 600 $\mu$ m (same as autograft macropores).

As a result of limited autologous bone availability and to minimise the problem of donor-site morbidity, many efforts have been made to find adequate supporting material for augmentation after osteotomy (Bauer et al., 2000; De Long et al., 2007). In this context, we chose biomaterials on base of calcium phosphates as solution for the biomedical applications. Thus,  $\beta$ -TCP or Hap-TCP combination has been clinically used to repair bone defects for many years (Elliott, 1994). Whereas,  $\beta$ -TCP or Hap-TCP have poor mechanical properties (Elliott, 1994; Wang et al., 2004). The usage at high load bearing conditions was restricted due to its brittleness, poor fatigue resistance and strength. Hence, there was a need for improving the mechanical properties of these materials by suitable biomaterials for clinical applications. We offer the study of the mixtures of tricalcium phosphate ( $\beta$ -TCP) and synthetic Fap in order to obtain a bioceramic with better mechanical properties than Hap-TCP combination or  $\beta$ -TCP as separately used. In fact, Fap is an attractive material due to its similarity in structure and bone composition in addition to the benefit of fluorine release (Elliott, 1994; Ben Ayed et al., 2001a). In Vitro studies we have shown that Fap is biocompatible (Elliott, 1994). It also has better stability and provides fluorine release at a controlled rate to ensure the formation of a mechanically and functionally strong bone (Elliott, 1994; Ben Ayed et al., 2006b).

Most studies have been devoted to the knowledge of the mechanical properties and biomedical applications of TCP-Hap (Elliott, 1994; Landi et al., 2000; Gutierrez et al., 2007). On the contrary little work has been devoted to the sintering, mechanical properties and clinical applications of TCP-Fap (Ben Ayed et al., 2007). So, the aim of this study is to prepare a biphasic calcium phosphates composites (tricalcium phosphate and fluorapatite) at various temperatures (between 1100°C and 1450°C) with different percentages of fluorine (0.5 wt %; 0.75 wt %; 1 wt %; 1.25 wt % and 1.5 wt % respectively, to the mass Fap percentage: 13.26 wt %; 19.9 wt %; 26.52 wt %; 33.16 wt % and 40 wt %). It also aims to characterize the resulting composites with density, mechanical resistance, infrared spectroscopy, X-ray diffraction, nuclear magnetic resonance ( $^{31}$ P) and scanning electron microscopy measurements.

## 2. Materials and methods

In this study the main used materials are commercial tricalcium phosphate (Fluka) and synthesized fluorapatite. The Fap powder was synthesized by the precipitation method (Ben Ayed et al., 2000). A calcium nitrate ( $\text{Ca}(\text{NO}_3)_2 \cdot 4\text{H}_2\text{O}$ , Merck) solution was slowly added to a boiling solution containing diammonium hydrogenophosphate ( $(\text{NH}_4)_2\text{HPO}_4$ , Merck) and ammonium fluoride ( $\text{NH}_4\text{F}$ , Merck), with continuous magnetic stirring. During the reaction, pH was adjusted to the same level (pH 8-9) by adding ammonia. The obtained precipitate was filtered and washed with deionised water; it was then dried at  $70^\circ\text{C}$  for 12h.

Estimated quantities of each powder ( $\beta$ -TCP and Fap) were milled with absolute ethanol and treated by ultra-sound machine for 15 min. The milled powder was dried at  $120^\circ\text{C}$  in a steam room to remove the ethanol and produce a finely divided powder. Powder mixtures were moulded in a metal mould and uniaxially pressed at 150 MPa to form cylindrical compacts with a diameter of 20 mm and a thickness of about 6 mm. The green bodies were sintered without any applied pressure or air at various temperatures (between  $1100^\circ\text{C}$  and  $1450^\circ\text{C}$ ). The heating rate was  $10^\circ\text{C min}^{-1}$ . The green compacts were sintered in a vertical resistance furnace (Pyrox 2408). The relative densities of the sintered bodies were calculated by the dimensions and weight. The relative error of densification value was about 1%.

The received powder was analyzed by using X-ray diffraction (XRD). The X-rays have used the Seifert XRD 3000 TT diffractometer. The X radiance was produced by using  $\text{CuK}_\alpha$  radiation ( $\lambda = 1.54056 \text{ \AA}$ ). The crystalline phases were identified from powder diffraction files (PDF) of the International Center for Diffraction Data (ICDD).

The samples were also submitted to infrared spectrometric analysis (Perkin-Elmer 783) using KBr.

Linear shrinkage was determined by dilatometry (Setaram TMA 92 dilatometer). The heating and cooling rates were  $10^\circ\text{C min}^{-1}$  and  $20^\circ\text{C min}^{-1}$ , respectively.

Differential thermal analysis (DTA) was carried out using about 30 mg of powder (DTA-TG, Setaram Model). The heating rate was  $10^\circ\text{C min}^{-1}$ .

The  $^{31}\text{P}$  magic angle spinning nuclear magnetic resonance ( $^{31}\text{P}$  MAS NMR) spectra were run on a Bruker 300WB spectrometer. The  $^{31}\text{P}$  observational frequency was 121.49 MHz with 3.0  $\mu\text{s}$  pulse duration, spin speed 8000 Hz and delay 5 s with 2048 scans.  $^{31}\text{P}$  shift is given in parts per million (ppm) referenced to 85 wt%  $\text{H}_3\text{PO}_4$ .

The microstructure of the sintered compacts was investigated by scanning electron microscope (Philips XL 30) on fractured sample surfaces. Because calcium phosphates are insulating biomaterial, the sample was coated with gold for more electronic conduction.

The particle size dimension of the powder was measured by means of Micromeritics Sedigraph 5000. The specific surface area (SSA) was measured by the BET method using azotes ( $\text{N}_2$ ) as an adsorption gas (ASAP 2010) (Brunauer et al., 1938). The main particle size ( $D_{\text{BET}}$ ) was calculated by assuming that the primary particles are spherical (Ben Ayed et al., 2001b):

$$D_{\text{BET}} = \frac{6}{s \cdot \rho} \quad (1)$$

Where  $\rho$  is the theoretical density of  $\beta$ -TCP ( $3.07 \text{ g.cm}^{-3}$ ) or Fap ( $3.19 \text{ g.cm}^{-3}$ ) and  $s$  is the SSA. The Brazilian test was officially considered by the International Society for Rock Mechanics (ISRM) as a method for determining the tensile strength of rock materials (ISRM, 1978). The Brazilian test was also standardised by the American Society for testing materials (ASTM) to

obtain the tensile strength of concrete materials (ASTM, 1984). The diametrical compression test also called the Brazilian disc test or the diametrical tensile test was considered a reliable and accurate method to determine the strength of brittle and low strength material.

An interesting parameter is the tensile strength,  $\sigma_r$ , which is the maximum nominal tensile stress value of the material. What is defined here is the horizontal tensile stress at the initiation of the large vertical crack at the centre of the disc. For the calculation of the tensile stress in the middle of the disc, Eq. (2) was used, corresponding to a plane stress condition. The usual way in evaluating the tensile strength from diametral compression test is by substituting the maximum load value into Eq. (2).

$$\sigma_r = \frac{P}{S} = \frac{2 \cdot P}{\Pi \cdot D \cdot t} \quad (2)$$

where P is the maximum applied load, D diameter, t thickness of the disc and  $\sigma_r$  the tensile strength (or mechanical strength).

The essays were realized by means of a device by using "LLOYD EZ50" on cylindrical samples of 6 mm approximately of thickness and 20 mm of diameter. At least six specimens were tested for each test condition. An average of the values was then calculated. The results dispersal is in the order of 15 %.

### 3. Results and discussion

#### 3.1 Characterization of powder

Table 1 shows the SSA of  $\beta$ -TCP powder, Fap powder and different  $\beta$ -TCP - Fap composites, the average grain size  $D_{BET}$  (calculated by equation (1)) and the particle size distribution data (measured by granulometric repartition). The difference between the value deduced by SSA and by granulometric repartition was probably due to the presence of agglomerates in the initial powder. The SSA of different  $\beta$ -TCP - Fap composites increases with the percentages of Fap whereas the average grain size decreases (Table 1). This result shows the effect of Fap additive in tricalcium phosphate matrix. Indeed, the grain of Fap has a dense morphology by report  $\beta$ -TCP, which was responsible of the increasing of different composites SSA.

Compound	SSA (m <sup>2</sup> /g) ± 1.00	$D_{BET}$ (µm) ± 0.20	$D_{50}$ (µm) <sup>(a)</sup> ± 0.20	$d^b$
Fap	29.00	0.07	6	3.190
$\beta$ -TCP	0.70	2.80	5	3.070 ( $\beta$ ) 2.860 ( $\alpha$ )
$\beta$ -TCP - 13.26 wt% Fap composites	2.90	0.67	-	3.086
$\beta$ -TCP - 19.90 wt% Fap composites	3.32	0.58	-	3.094
$\beta$ -TCP - 26.52 wt% Fap composites	3.80	0.51	-	3.101
$\beta$ -TCP - 33.16 wt% Fap composites	4.37	0.44	-	3.110
$\beta$ -TCP - 40 wt% Fap composites	5.24	0.36	-	3.118

<sup>a</sup> : Mean diameter, <sup>b</sup> : theoretical density.

Table 1. SSA and average grain size obtained by different analysis of various compounds.

Fig. 1 shows the dilatometric measurements of a different powder used in this study ( $\beta$ -TCP, Fap and different  $\beta$ -TCP-Fap composites). The sintering temperatures began at about

1180°C, 1154°C, 1145°C, 1100°C, 1052°C, 1045°C and 775°C for  $\beta$ -TCP,  $\beta$ -TCP - 13.26 wt% Fap composites,  $\beta$ -TCP - 19.90 wt% Fap composites,  $\beta$ -TCP - 26.52 wt% Fap composites,  $\beta$ -TCP - 33.16 wt% Fap composites,  $\beta$ -TCP - 40 wt% Fap composites and Fap, respectively. The addition to Fap additive in the matrix of  $\beta$ -TCP decreasing the sintering temperature of the pure tricalcium phosphate (Fig. 1b-1f). Indeed, the sintering temperature of  $\beta$ -TCP decreases when the percentage of Fap increases.

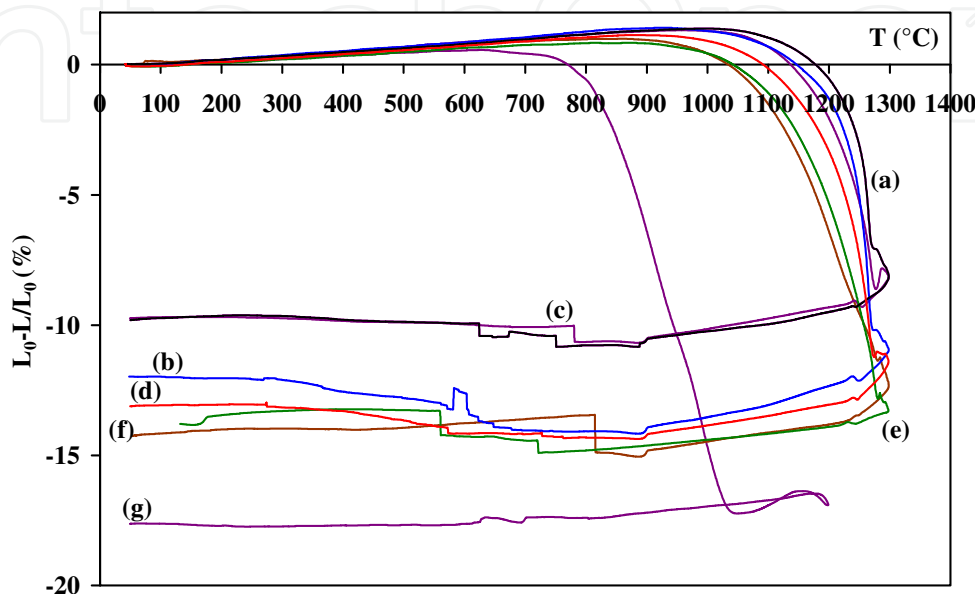


Fig. 1. Linear shrinkage versus temperature of: (a)  $\beta$ -TCP powder, (b)  $\beta$ -TCP - 13.26 wt% Fap composites, (c)  $\beta$ -TCP - 19.9 wt% Fap composites, (d)  $\beta$ -TCP - 26.52 wt% Fap composites, (e)  $\beta$ -TCP - 33.16 wt% Fap composites, (f)  $\beta$ -TCP - 40 wt% Fap composites, (g) Fap powder.

Differential thermal analysis studies detected out a potential phase change during the sintering of a different powder used in this study. Fig. 2a shows DTA curve of  $\beta$ -TCP. The DTA thermogramme shows 2 peaks relatives to the first and second endothermic allotropic transformation of  $\beta$ -TCP (1290°C and 1464°C). The last endothermic peak, at 1278°C, was related to a peritectic between  $\beta$ -TCP and pyrophosphate ( $\beta$ -Ca<sub>2</sub>P<sub>2</sub>O<sub>7</sub>). The chemical reaction was illustrated in the following:



This was similar to the result previously reported by Destainville and colleagues (Destainville et al., 2003).

Fig. 2b and Fig. 2g show the DTA curves of  $\beta$ -TCP - 13.26 wt% Fap composites and Fap powder, respectively. We notice one endothermic peak around 1180°C. This peak may be due to the formation of a liquid phase, formed from binary eutectic between CaF<sub>2</sub> and Fap (Ben Ayed et al., 2000). We can assume that fluorite (CaF<sub>2</sub>) was formed as a second phase during the powder preparation of Fap.

Fig. 2c, 2e and 2f illustrate the DTA curves of  $\beta$ -TCP - 19.9 wt% Fap composites,  $\beta$ -TCP - 33.16 wt% Fap composites and  $\beta$ -TCP - 40 wt% Fap composites, respectively. Fig. 2c and 2f are practically similar with the Fig. 2a. Indeed, DTA thermogramme of composites shows also 2 peaks of tricalcium phosphate allotropic transformations.

The DTA thermogramme of TCP - 26.52 wt% Fap composites shows 3 endothermic peaks at 1268°C, at 1280°C and at 1444°C, which are two peaks related with two allotropic transformations of tricalcium phosphate (Fig. 2d). The temperatures of allotropic transformations have been decreased about 10°C (1280°C in the place 1290°C) and 20°C (1444°C in the place 1464°C) with that of the pure  $\beta$ -TCP. This result has been explained probably by the Fap effect in  $\beta$ -CTCP matrix.

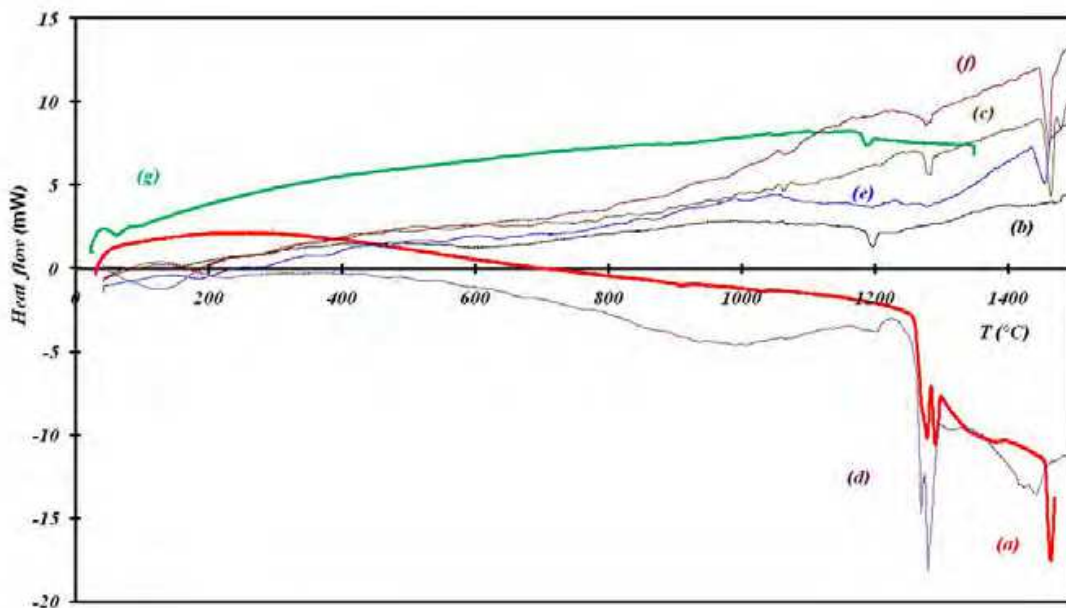


Fig. 2. DTA curves of: (a)  $\beta$ -TCP powder, (b)  $\beta$ -TCP - 13.26 wt% Fap composites, (c)  $\beta$ -TCP - 19.9 wt% Fap composites, (d)  $\beta$ -TCP - 26.52 wt% Fap composites, (e)  $\beta$ -TCP - 33.16 wt% Fap composites, (f)  $\beta$ -TCP - 40 wt% Fap composites, (g) Fap powder.

The DTA thermogrammes of  $\beta$ -TCP - 33.16 wt% Fap composites and  $\beta$ -TCP - 40 wt% Fap composites show only 2 endothermic peaks, which are relative to the allotropic transformations of tricalcium phosphate (Fig. 2e and 2f). In these curves, the endothermic peak relative to a peritectic between  $\beta$ -TCP and  $\beta$ - $\text{Ca}_2\text{P}_2\text{O}_7$  is practically disappeared. This chemical reaction between tricalcium phosphate and pyrophosphate was improved by the addition of 33.16 wt% or more Fap. Also, the temperatures of allotropic transformations decreased when the percentage of Fap increases (Fig. 2c-2f). This result has been explained probably by the Fap effect in  $\beta$ -TCP matrix.

### 3.2 Sintering and mechanical properties of tricalcium phosphate – fluorapatite composites

This Table 2 summarizes the mechanical strength of different  $\beta$ -TCP sintered at various temperatures (1100°C-1450°C) with different amounts of Fap (13.26 wt%, 19.9 wt%, 26.52 wt, 33.16 wt% and 40 wt%).

Fig. 3 illustrates the evolution of density and rupture strength of the composites sintered for 1h at various temperatures (between 1100°C and 1450°C) at different percentages of Fap (13.26 wt %; 19.9 wt %; 26.52 wt %; 33.16 wt % and 40 wt %). The densification and mechanical resistance varied as a function of Fap in the  $\beta$ -TCP matrix and sintering temperature.

wt% Fap	13.60	19.90	26.52	33.16	40.00
T (°C)	$\sigma_r$ (MPa)				
1100	0.25	1.68	2.00	2.53	0.23
1150	0.50	2.11	2.20	2.73	0.54
1200	0.90	2.55	3.00	3.01	0.85
1250	1.36	2.86	3.80	6.23	1.33
1300	2.31	3.41	6.00	8.74	1.80
1320	3.80	6.10	8.00	9.80	4.50
1350	6.00	6.45	9.20	13.20	10.10
1400	7.10	7.10	9.60	13.70	11.80
1450	3.60	5.33	8.00	5.70	6.20
Green	0.10	0.20	0.20	0.30	0.20

Table 2. Rupture strength versus temperature of different TCP-Fap composites.

Fig. 3A shows the relative density and mechanical resistance of  $\beta$ -TCP - 13.26 wt% Fap composites. The rupture strength and densification increase with sintering temperature. The optimum densification was obtained at 1350°C (87%). The maximum mechanical resistance reached 7.1MPa at 1400°C (Fig. 3A). This study shows that small additions of a Fap (13.26 wt %) can significantly enhance the sinterability and strength of  $\beta$ -TCP.

The evolution of  $\beta$ -TCP - 19.90 wt% Fap composites of densification and mechanical properties was practically similar to the  $\beta$ -TCP sintered with 13.26 wt% Fap (Fig. 3B). This curve illustrates a maximum densification at about 89% corresponding to the composites sintered at 1350°C. The mechanical resistance was similar to the  $\beta$ -TCP - 13.26 wt% Fap composites in value and sintering temperature (7.1 MPa at 1400°C).

Fig. 3C illustrates the evolution of the composites densification relative to the temperature between 1100°C and 1450°C. The densification was variable as a function of temperature. Between 1100°C and 1200°C, the samples relatives' densities were very small for any samples. An increase of density was shown between 1300°C and 1400°C, where the optimum densities are about 89.1 % at 1350°C. Fig. 3C shows the mechanical properties of the  $\beta$ -TCP - 26.52 wt% Fap composites samples according to the sintering temperature. Between 1100°C and 1250°C, the rupture strength of TCP - 26.52 wt% Fap composites samples was around 2-3 MPa. Above 1250°C, the rupture strength increases and reaches maximum value at 1400°C (9.6 MPa). Above 1400°C, the mechanicals properties of composites decrease during the sintering process. Indeed, the mechanical resistance of TCP - 26.52 wt % Fap composites reaches the 8 MPa at 1450°C. The evolution of mechanical properties of composites was considered a function of a sintering temperature. At 1350°C, the mechanical resistance optimum of  $\beta$ -TCP sintered without Fap additive reached 5.3 MPa (Bousslama et al., 2009), whereas the resistance increases to 9.4 MPa with 26.52 wt% Fap.



Fig. 3D shows the results of densification and mechanical properties of  $\beta$ -TCP - 33.16 wt% Fap composites. The ultimate densification was obtained at 1350°C (93.2%) and the maximum of mechanical resistance was approached at 1400°C (13.7 MPa). The  $\beta$ -TCP - Fap composites ratio was strongly dependent on the percentage Fap addition. The densification and mechanical properties remain low with 13.26 wt% Fap and 19.90 wt% Fap, when  $\beta$ -TCP sintered with 33.16 wt % Fap, the densification and mechanical resistance increase with the sintering temperature and reaches its maximum values.

With 40 wt % Fap, the densification and mechanical resistance decrease slowly with sintering temperature (Fig. 3E). The optimum relative density was obtained at 1350°C (92%) and the maximum mechanical resistance reached at 1400°C (11.8 MPa). As the amount of Fap increased (40 wt %), sinterability and mechanical properties considerably decreased. This result was clarified by the large (increase weight ratio) amounts of Fap used in the prepared composites. In fact the microstructure and thermal properties of Fap weren't stable at high temperature (after 1300°C) (Ben Ayed et al., 2000 and 2001b). Above 1400°C, the densification and the mechanical properties decrease with any  $\beta$ -TCP sintered with different percentages of Fap (Fig. 3).

Table 3 summarizes the optimum values of density and mechanical resistance of  $\beta$ -TCP sintered for 1h with different percentages of Fap. Whatever the content of Fap, the maximum of densification was obtained at 1350°C, whereas the optimum of rupture strength was reached at 1400°C (Table 3). The optimum values were obtained for  $\beta$ -TCP sintered with 33.16 wt% Fap (93.2% and 13.7 MPa).

wt % Fap	13.26	19.90	26.52	33.16	40
Optimum density (%)	87.87	89.00	89.10	93.20	92.62
Optimum strength (MPa)	7.1	7.1	9.6	13.7	11.8

Table 3. Optimum values of density (at 1350°C) and mechanical resistance (at 1400°C) of different  $\beta$ -TCP-Fap composites.

An increase of  $\beta$ -TCP- Fap density was shown between 1300°C and 1400°C, where the optimum densities were obtained at 1350°C with 33.16 wt % Fap. The used temperatures are similar to the densification of tricalcium phosphate when singly used (Ben Ayed et al., 2006a). But, the temperatures are relatively higher in comparison to those used for densification of only Fap (Ben Ayed et al., 2000, 2001b and 2006b). Indeed, Fap presents a good sinterability in the temperature ranging at 900°C-1100°C (Ben Ayed et al., 2000 and 2001b). At 1450°C, the densities decrease at different degrees of Fap additions. These results are similar to the previously reported by Ben Ayed et al. during the study of elaboration and characterization of calcium phosphate biomaterial (Ben Ayed et al., 2007).

This study shows the mechanical properties of the  $\beta$ -TCP-Fap composites samples according to the sintering temperature. At lower temperature (between 1100°C and 1200°C), the rupture strength of  $\beta$ -TCP-Fap composites was around 1 and 3 MPa (Fig. 3). When sintering temperature increase above 1200°C, the rupture strength increases slowly. These results are due to the increase of the densification caused by the growth of the grains size. Beyond 1300°C, the rupture strength increases and reaches maximum value at 1400°C. Between 1350°C and 1400°C, the increase in rupture strength was very clear for all samples with different weight ratio of Fap in the composites specimens. This is attributed to the influence and effect of Fap additive in relative densities and mechanical properties of the sintered composites. In fact, Ben Ayed et al. show that Fap has a good sinterability and mechanical

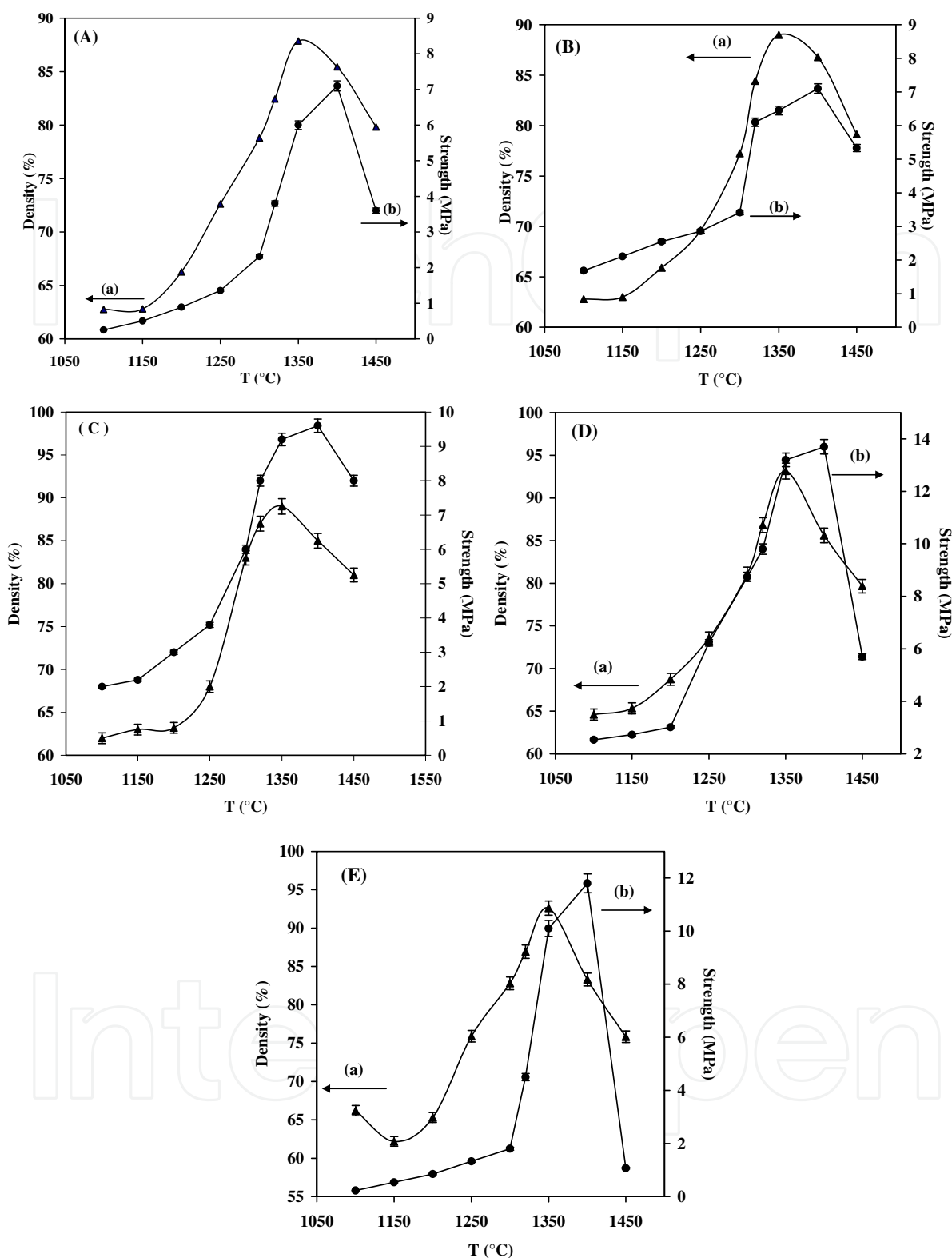


Fig. 3. Density and mechanical strength versus temperature of  $\beta$ -TCP sintered for one hour with different wt % of Fap: (A):  $\beta$ -TCP - 13.26 wt% Fap composites, (B)  $\beta$ -TCP - 19.90 wt% Fap composites, (C)  $\beta$ -TCP - 26.52 wt% Fap composites, (D)  $\beta$ -TCP - 33.16 wt% Fap composites, (E)  $\beta$ -TCP - 40 wt% Fap composites, ((a) : Density, (b): strength).

resistance (Ben Ayed et al., 2006b). It revealed that the mechanical resistance increases with temperature and reaches its maximum value about 14 MPa (Ben Ayed et al., 2006b).

The mechanical properties of the  $\beta$ -TCP and different TCP - Fap composites depend directly on the properties of the departure powder (granulometric, crystallinity of the powder, chemical composition, origin of powder) and on the operative conditions of the sintering process (temperature, heating time, cycle of sintering, atmosphere) (Ben Ayed et al., 2006b). Each of these parameters has a direct effect on the final properties of the composite.

Resorbable beta-tricalcium phosphate bioceramic is known for its excellent biocompatibility. However, it exhibits poor tensile strength. Here, we improved tensile strength of  $\beta$ -TCP bioceramic without altering its biocompatibility by introducing Fap additives, in different quantities (13.26 wt %; 19.9 wt %; 26.52 wt %; 33.16 wt % and 40 wt %). In this study, we showed that the presence of Fap with different amounts in  $\beta$ -TCP matrix improves the mechanical properties of  $\beta$ -TCP-Fap composites. This result was similar to the previous report by Bouslama et al. (Bouslama et al., 2009).

Table 4 displays several examples of dense calcium phosphates composites mechanical properties. The values found by mechanical strength were unequalled with the values in Table 4, because the authors have used different mechanical modes others than the Brazilian test. Indeed, many factors influence the mechanical properties such as: initial materials, the process conditions and annealing treatment. So, it is difficult to compare the results of this study with those found in literature.

Materials	$\sigma_r$ (MPa) <sup>a</sup>	$\sigma_f$ (MPa) <sup>b</sup>	$\sigma_c$ (MPa) <sup>c</sup>	$K_{1C}$ (GPa) <sup>d</sup>	References
Fap	14.00	-	-	4.5	Ben Ayed et al., 2006b
$\beta$ -CTCP	5.30	-	-	-	Bouslama et al., 2009
$\beta$ -TCP	-	92.00	-	-	Kalita et al., 2008
$\beta$ -TCP- Fap composites	9.60	-	-	-	Bouslama et al., 2009
brushite	-	-	32.00	-	Hofmann et al., 2009
Hap	-	-	5.35	3.52	Balcik et al., 2007
TCP-Hap composites (40/60)	-	-	4.89	3.10	Balcik et al., 2007
Hap- poly-L-lactic acid composites	-	-	100.00	6.00	Gay et al., 2009

<sup>a</sup> $\sigma_r$ : Mechanical strength (Brazilian test), <sup>b</sup> $\sigma_f$ : Flexural strength, <sup>c</sup> $\sigma_c$ : Compressive strength, <sup>d</sup> $K_{1C}$ :Young's modulus.

Table 4. Literature examples of dense calcium phosphates composites mechanical properties.

### 3.3 Characterization of sintered tricalcium phosphate - fluorapatite composites

After sintering, different techniques characterized the samples: X rays diffraction (XRD), <sup>31</sup>P MAS-NMR, scanning electronic microscopy (SEM) and infrared spectroscopy (IR).

Composites of  $\beta$ -TCP with Fap were pressureless sintered at temperatures from 1100 to 1450°C. The reactions and transformations of phases were monitored with X-ray diffraction.

The XRD patterns of the  $\beta$ -TCP were sintered at various temperatures (1100°C, 1300°C and 1400°C) with different percentages of Fap (13.26 wt % and 40 wt %) were shown in Fig. 4. These spectra are identical to the initial powder ( $\beta$ -TCP and Fap). We conclude that  $\beta$ -TCP and the Fap were steady during the sintering process. But when left at 1300°C, the thermogrammes indicate the germination of  $\alpha$ -TCP phase. This phase is a proof of the fragility of samples because the absolute densities of  $\beta$ -TCP and  $\alpha$ -TCP were different. Besides, the incorporation of Fap in tricalcium phosphate does not seem to be in its right decomposition. Indeed, the XRD revealed only phases of departure ( $\beta$ -TCP and Fap) and  $\alpha$ -TCP.

The Nuclear magnetic resonance chemical shift spectra of the  $^{31}\text{P}$  of the  $\beta$ -TCP as sintered at various temperatures (1100°C; 1300°C and 1400°C) with different percentages of Fap (13.26 wt %; 33.16 wt % and 40 wt %) are shown in Fig. 5. The  $^{31}\text{P}$  MAS-NMR solid spectra of composites show the presence of three tetrahedral environments of the phosphorus. Indeed, the  $^{31}\text{P}$  MAS - NMR analysis reveals the presence of three tetrahedral P sites for the  $\beta$ -TCP whereas the Fap possesses only one. This was similar to the result previously reported by (Yashima et al., 2003). They show that the phosphorus of tricalcium phosphate is located in three crystallographic sites: P(1)O<sub>4</sub>, P(2)O<sub>4</sub>, P(3)O<sub>4</sub> (Yashima et al., 2003). There is no record of any phase modification of the  $\beta$ -TCP or Fap, which confirms that the two powders,  $\beta$ -TCP and Fap were thermally steady between 1100°C and 1450°C.

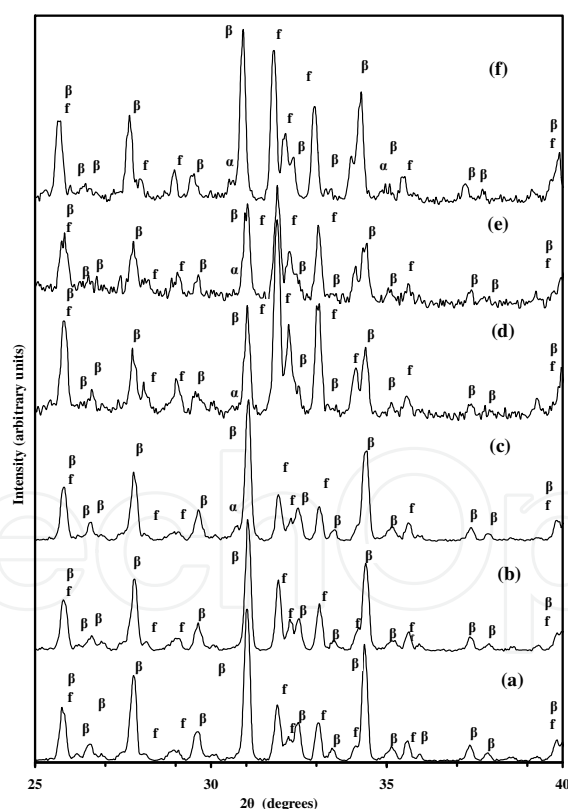


Fig. 4. XRD patterns of  $\beta$ -TCP-Fap composites sintered for one hour at various temperatures with different wt % of Fap: (a) 13.26 wt %, 1100°C; (b) 13.26 wt %, 1300°C; (c) 13.26 wt %, 1400°C; (d) 40 wt %, 1100°C; (e) 40 wt %, 1300°C and (f) 40 wt %, 1400°C ( $\beta$  :  $\beta$ -TCP; f: Fap;  $\alpha$  :  $\alpha$ -TCP).

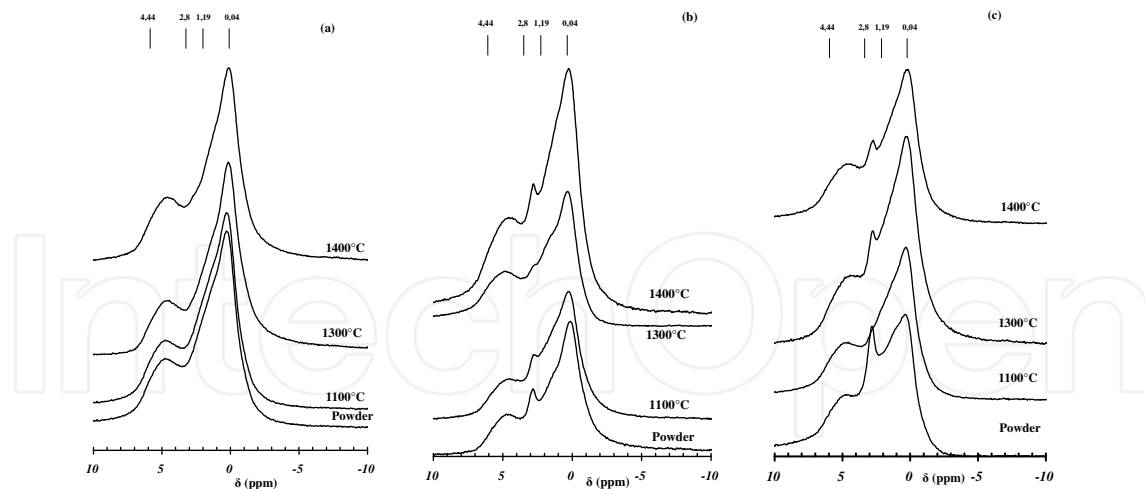
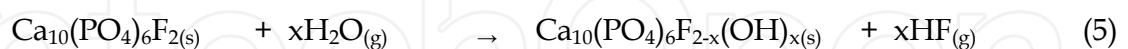


Fig. 5.  $^{31}\text{P}$  NMR spectra of  $\beta$ -TCP-Fap composites sintered for one hour at various temperatures with different wt % of Fap : (a) 13.26 wt %; (b) 33.16 wt % and (c) 40 wt % ( $\beta$  :  $\beta$ -TCP; f: Fap).

Fig. 6 and Fig. 7 show the SEM micrographs of  $\beta$ -TCP-Fap composites. This technique helps to investigate the texture and porosity of the biphasic bioceramic. The fracture surfaces clearly show the composite as sintered at various temperatures (1100°C, 1300°C, 1400°C and 1450°C) with different percentages of Fap (13.26 wt %; 19.9 wt %; 33.16 wt % and 40 wt %) revealing the influence of the temperature of microstructural developments during the sintering process (Fig. 6). These effects increased along the sintering temperature and the percentage of Fap.

The results of microstructural investigations of  $\beta$ -TCP-Fap composites sintered at various temperatures (1100°C and 1450°C) with 13.26 wt % Fap are shown in Fig. 6a and b. At 1100°C, the sample presents an important intergranular porosity (Fig. 6a). At higher temperatures (1450°C), the densification was hindered by the formation of large pores (Fig. 6b). During the sintering of Fap and TCP-Fap composites, Ben Ayed et al. also observed the formation of large pores at these temperatures (Ben Ayed et al., 2001b). They are attributed to the hydrolysis of Fap and  $\text{CaF}_2$ , as expressed by the following equation:



The increase of percentages of Fap from 13.26 wt % to 19.9 wt % did not show a significant change of the microstructure. When temperature increases, the microstructure of  $\beta$ -TCP-Fap composites was sintered at 1300°C with different percentages of Fap (19.90 wt %; and 33.16 wt %) reveals moderate grain growth (Fig. 6c and d). Indeed, we notice a partial reduction of the porosity and a presence of some closed pores (Fig. 6c and d).

At 1400°C, the microstructural analysis of  $\beta$ -TCP- 40 wt% Fap composites reveals the creation of a liquid phase (Fig. 6e). The outstanding modification on the microstructure of  $\beta$ -TCP-Fap composites takes place only due to the presence of a liquid phase that can occur by the increase of the sintering temperature or by an increase of the Fap content (Fig. 6e). At this temperature (1400°C), the fragility and the decrease of relative densities and mechanical properties were originated from the micro-crack formed by small expansion of the phase transformation samples due to the low density of  $\alpha$ -TCP (2.86 g/cm<sup>3</sup>) than that of  $\beta$ -TCP (3.07 g/cm<sup>3</sup>) (Fig. 6e). But also from the allotropic transformation from  $\beta$  to  $\alpha$  and from  $\alpha$  to  $\alpha'$ .

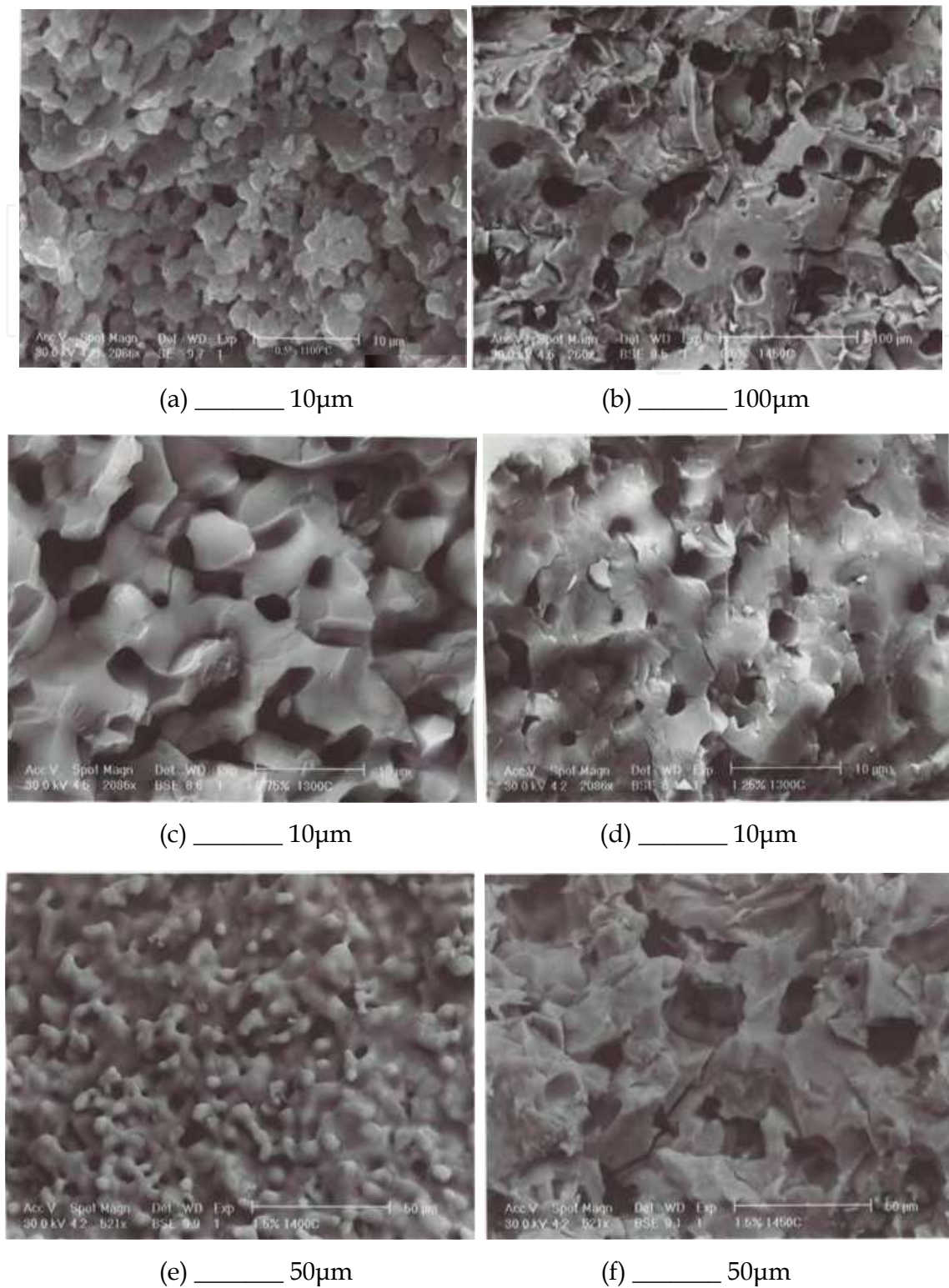


Fig. 6. SEM micrograph (fracture) of  $\beta$ -TCP-Fap composites sintered for one hour at various temperatures with different wt % of Fap: (a) 13.26 wt %, 1100°C; (b) 13.26 wt %, 1450°C; (c) 19.9 wt %, 1300°C; (d) 33.16 wt %, 1300°C; (e) 40 wt %, 1400°C and (f) 40 wt %, 1450°C.

Above 1400°C, the microstructure of  $\beta$ -TCP sintered at 1450°C with different percentages of Fap (13.26 wt % and 40 wt %) was totally modified (Fig. 6b and f). In fact, we observe two

types of microstructures; the first was characterized by the creation of large pores engendering the reaction of hydrolysis of Fap and the second was characterized by the exaggerated coarsening of grains (Fig. 6b and f). The microstructural analysis of the composite shows a larger amount of pores, preferentially located on the grain boundaries. In Fig. 7, the fracture surfaces show clearly the  $\beta$ -TCP-26.52 wt% Fap composite as sintered for 1 h at various temperatures (1300, 1350, 1400 and 1450°C) revealing the influence of the temperature of microstructural developments during the sintering process. These effects increased along the sintering temperature. The results of microstructural investigations of  $\beta$ -TCP-26.52 wt% Fap composites show that the morphology of the samples was completely transformed (Fig. 7a-d).

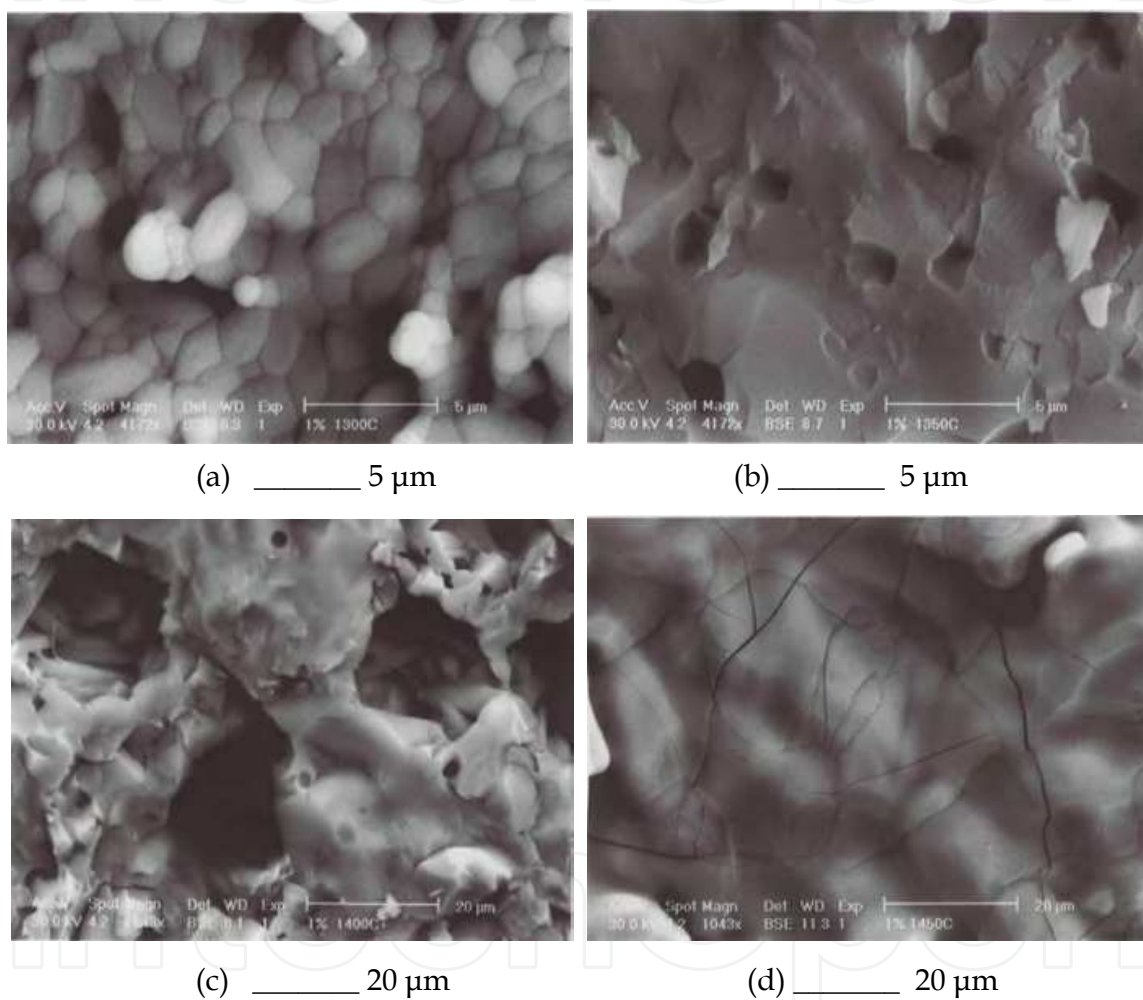
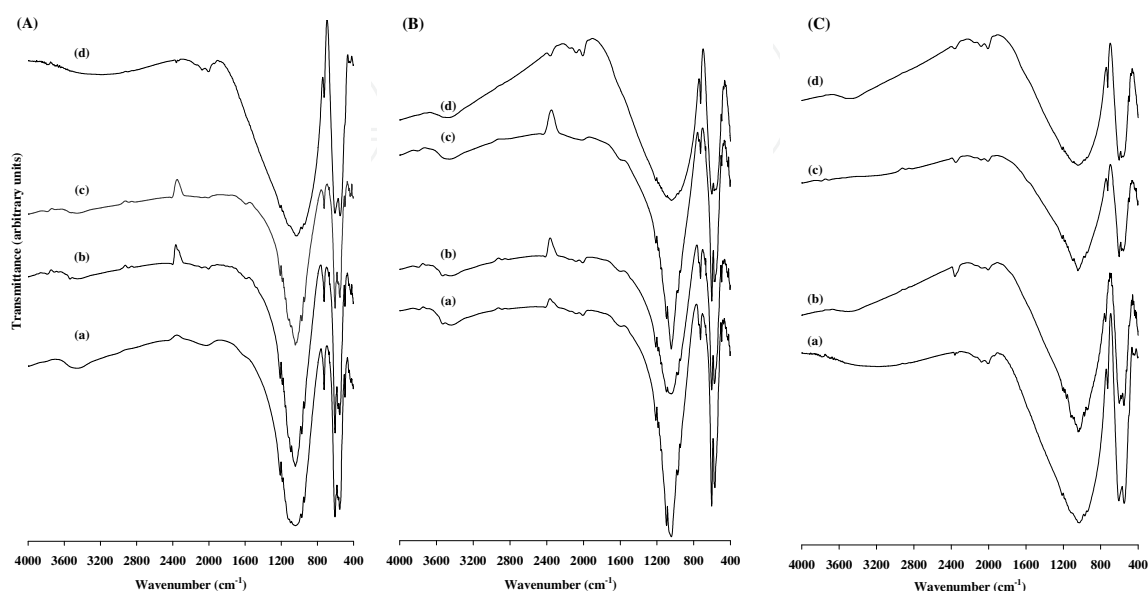


Fig. 7. SEM micrograph of  $\beta$ -TCP - 26.52 wt% Fap composites sintered for 1h at: (a) 1300°C, (b) 1350°C, (c) 1400°C, (d) 1450°C.

At 1300°C, the SEM micrographs of samples show liquid phase relative to the binary peritectic between pyrophosphate with the tricalcium phosphate (Fig. 7a). At 1350°C, one notices a partial reduction of the porosity (Fig. 7b). At higher temperatures (1400-1450°C), the densification was hindered by the formation of both large pores and many cracks (Fig. 7c and d).

Fig. 8A-8B show typical IR spectra of  $\beta$ -TCP sintered for one hour at various temperatures (1100°C, 1200°C, 1300°C and 1400°C) with 13.26 wt% and 40 wt% Fap, respectively. Most

bands were characteristic of phosphate group of  $\beta$ -TCP and Fap (at 540-600  $\text{cm}^{-1}$  and 920-1120  $\text{cm}^{-1}$ ). The peaks at 920  $\text{cm}^{-1}$  and 1120  $\text{cm}^{-1}$  are assigned to the stretching vibration of  $\text{PO}_4^{3-}$  ions and the peaks at 540  $\text{cm}^{-1}$  and 600  $\text{cm}^{-1}$  are assigned to the deformation vibration of  $\text{PO}_4^{3-}$  ions. The bands at 3500  $\text{cm}^{-1}$  and at 1640  $\text{cm}^{-1}$  were assigned to the adsorbed water molecule.



(A) with 13.26 wt% Fap at various temperatures: (a) 1100°C, (b) 1200°C, (c) 1300°C and (d) 1400°C.  
 (B) with 40 wt% Fap at various temperatures: (a) 1100°C, (b) 1200°C, (c) 1300°C and (d) 1400°C.  
 (C) at 1400°C with different percentages of Fap: (a) 13.26 wt %; (b) 19.9 wt %; (c) 33.16 wt % and (d) 40 wt%.

Fig. 8. IR of  $\beta$ -TCP sintered for one hour

Figs. 8A(a-b), 8B(a-b) show the IR spectra of the  $\beta$ -TCP-Fap composites sintered at 1100°C and 1200°C, respectively. In the spectra absorptions assigned to OH group, are detected at 3510  $\text{cm}^{-1}$  and 747  $\text{cm}^{-1}$ . Those absorptions indicate that the OH group substitutes F in the Fap structure, thus leading to the formation of hydroxyfluorapatite ( $\text{Ca}_{10}(\text{PO}_4)_6\text{F}_{2-x}(\text{OH})_x$ : FOHap). This compound may be the result of the reaction between Fap and water vapour traces (Ben Ayed et al., 2001b). This reaction was illustrated by Eq. 5. At higher temperature (1300°C-1400°C), the intensity of these bands decreases but does not completely vanish supposing that the amount of fluoride in the samples decreases when the temperature increases (Figs. 8A(c-d), 8B(c-d)). IR spectra of different composites sintered at 1400°C with different percentages of Fap (13.26 wt %; 19.9 wt %; 33.16 wt % and 40 wt %) were practically similar to the Figs. 8A-8B. Indeed, the typical IR spectra show the characteristics of the phosphate group of calcium phosphates (at 500-600  $\text{cm}^{-1}$ , 1019  $\text{cm}^{-1}$ , 1034  $\text{cm}^{-1}$ , 1105  $\text{cm}^{-1}$ ).

At higher temperatures, the  $\beta$ -TCP-Fap composites densification and mechanical properties were hindered by the exaggerated grain growth, the effect of the allotropic transformation of  $\beta$ -TCP and the formation of intragranular porosity. The SEM micrograph illustrated the change of microstructure at 1450°C. These results are similar to the previously obtained by Ben Ayed et al. during the sintering process of TCP-Fap composites (Ben Ayed et al., 2007).



The preliminary results obtained in this study have shown that the  $\beta$ -TCP-Fap composites have a potential of further development into an alternative system to produce denser  $\beta$ -TCP bodies. Further investigations are still under way to investigate the influence of Fap on the density, microstructure and mechanical properties of  $\beta$ -TCP-Fap biomaterials.

#### 4. Conclusion

Tricalcium phosphate and fluorapatite powder were mixed in order to elaborate biphasic composites. The influence of Fap substitution on the  $\beta$ -TCP matrix was detected in the mechanical properties of the sintered composites. The characterization of samples was investigated by using X-Ray diffraction, differential thermal analysis, scanning electronic microscopy and by an analysis using  $^{31}\text{P}$  nuclear magnetic resonance. The sintering of tricalcium phosphate with different percentages of fluorapatite indicates the evolution of the microstructure, densification and mechanical properties. The Brazilian test was used to measure the rupture strength of biphasic composites biomaterials. The mechanical properties increase with the sintered temperature and with fluorapatite additive. The mechanical resistance of  $\beta$  tricalcium phosphate - 33.16 wt % fluorapatite composites reached its maximum value (13.7MPa) at 1400°C, whereas the optimum densification was obtained at 1350°C (93.2%). Above 1400°C, the densification and mechanical properties were hindered by the tricalcium phosphate allotropic transformation and the formation of both intragranular porosity and cracks.

#### 5. Acknowledgment

The author thanks the Professor Bouaziz Jamel and Doctor Bouslama Nadhem for their assistances in this work.

#### 6. References

- Aryee, S., Imhoff, A. B., Rose, T., Tischer, T., 2008. *Biomaterials*, 29, 3497-3502.
- Agneskirchner, J.D., Freiling, D., Hurschler, C., Lobenhoffer, P., 2006. *Knee Surg. Sports Traumatol Arthrosc*, 14, 291-300.
- ASTM C496, *Standard test method for splitting tensile strength of cylindrical concrete specimens Annual Book of ASTM Standards*, vol. 0.042, ASTM, Philadelphia, 1984, p. 336.
- Brouwer, R.W., Bierma-Zeinstra, S.M., van Raaij, T.M., Verhaar, J.A., 2006. *J. Bone Joint. Br.*, 454-9.
- Bauer, T.W., Muschler, G.F., *Bone graft materials. An overview of the basic science*, 2000. *Clin. Orthop. Relat. Res.*, 10-27.
- Balcik, C., Tokdemir, T., Senkoylo, A., Koc, N., Timucin, M., Akin, S., Korkusuz, P., Korkusuz, F., 2007. *Acta Biomaterialia*, 3, 985-996.
- Ben Ayed, F., Bouaziz, J., Bouzouita, K., 2000. *J. Eur. Ceram. Soc.* 20 (8), 1069.
- Ben Ayed, F., Bouaziz, J., Khattech, I., Bouzouita, K., 2001a. *Ann. Chim. Sci. Mater.* 26 (6), 75.
- Ben Ayed, F., Bouaziz, J., Bouzouita, K., 2001b. *J. Alloys Compd.* 322 (1-2), 238.
- Ben Ayed, F., Chaari, K., Bouaziz, J., Bouzouita, K., 2006a. *C. R. Physique* 7 (7), 825.
- Ben Ayed, F., Bouaziz, J., Bouzouita, K., 2006b. *Ann. Chim. Sci. Mater.* 31 (4), 393.

- Ben Ayed, F., Bouaziz, J., 2007. *C. R. Physique* 8 (1), 101-108.
- Ben Ayed, F., Bouaziz, J., 2008a. *Ceramics Int.* 34 (8), 1885-1892.
- Ben Ayed, F., Bouaziz, J. 2008b. *J. Eur. Ceram. Soc.* 28 (10), 1995-2002.
- Brunauer, S., Emmet, P. H., Teller, J., 1938. *Amer. Chem. Soc. J.* 60, 310.
- Bouaslama, N., Ben Ayed F., Bouaziz, J., 2009. *Ceramics Int.* 35, 1909-1917.
- Chaari, K., Ben Ayed F., Bouaziz, J., Bouzouita, K., 2009. *Materials Chemistry and Physics*, 113, 219-226.
- Destainville, A., Champion E., Bernache - Assolant, D., 2003. *Mater. Chem. Phys.* 80, 69.
- De Long, Jr. W.G., Einhorn, T.A., Koval, K., McKee, M., Smith, W., Sanders, R., 2007. *J. Bone Joint. Am.*, 89, 49-58.
- DeSilva, G.L., Fritzler, A., DeSilva, S.P., 2007. *Tech. Hand Up Extrem Surg.*, 11,163-7.
- Elliott, J. C., 1994. *Structure and Chemistry of the Apatite and Other Calcium Orthophosphates*, Elsevier Science B.V., Amsterdam.
- Fellah, B.H., Gauthier, O., Weiss, P., Chappard, D., Layrolle, P., 2008. *Biomaterials*, 29, 1177-88.
- Gaasbeek, R.D., Toonen, H.G., van Heerwaarden, R.J., Buma, P., 2005. *Biomaterials*, 26, 6713-9.
- Gutierrez, M., Dias, A.G., Lopes, M.A., Hussain, N.S., Cabral, A.T., Almeida, L., 2007. *J. Mater. Sci. Mater. Med.*, 18, 2377-82.
- García-Leiva, M.C., Ocaña, I., Martín-Meizoso, A., Martínez-Esnaola, J.M., 2002. *Engineering Fracture Mechanics* 69, 1007-1013.
- Gay, S., Arostegui, S., Lemaitre, J., 2008. *Materials Science and Engineering C*, in press.
- Hench, L. L., 1991. *J. Am. Ceram. Soc.* 74 (7), 1487.
- Hofmann, M.P., Mohammed, A.R., Perrie, Y., Gbureck, U., Barralet, J.E., 2009. *Acta Biomaterialia*, 5, 43-49.
- Hernigou, P., Ma, W., 2001. *Knee*, 8, 103-10.
- Hoell, S., Suttmoeller, J., Stoll, V., Fuchs, S., Gosheger, G., 2005. *Arch. Trauma Surg.*, 125, 638-43.
- ISRM. Suggested methods for determining tensile strength of rock materials, *Int. J. Rock Mech. Min. Sci. Geomech. Abstr.* 1978. 15, 99.
- Jensen, S.S., Broggini, N., Hjorting-Hansen, E., Schenk, R., Buser, D. 2006. *Clin. Oral. Implants Res.*, 17, 237-43.
- Kalita, S.J., Fleming, R., Bhatt, H., Schanen, B., Chakrabarti, R., 2008. *Materials Science and Engineering C*, 28, 392 - 398.
- Landi, E., Tampieri, A., Celotti, G., Sprio, S., 2000. *J. Eur. Ceram. Soc.* 20, 2377.
- Legeros, R. Z., 1993. *Clinical Materials* 14, 65.
- Okuda, T., Ioku, K., Yonezawa, I., Minagi, H., Kawachi, G., Gonda, Y., 2007. *Biomaterials*, 28, 2612-21.
- Steffen, T., Stoll, T., Arvinte, T., Schenk, R.K., 2001. *Eur. Spine J.*, 10 (Suppl 2), 132-40.
- Schilling, A.F., Linhart, W., Filke, S., Gebauer, M., Schinke, T., Rueger, J.M., 2004. *Biomaterials*, 25, 3963-72.
- Uwe, P., Angela, E., Christian, R., 1993. *Mater. J. Sci.: Mate In Medicine* 4, 292.
- Varma, H. K., Sureshbabu, S. 2001. *Materials letters* 49, 83.

Wang, C. X., Zhou, X., Wang, M. 2004. *Materials Characterization* 52, 301.

Yashima, M., Sakai, A. , Kamiyama, T., Hoshikawa, A., 2003. *J. Solid State Chemistry* 175, 272.

IntechOpen

IntechOpen



## **Biomaterials - Physics and Chemistry**

Edited by Prof. Rosario Pignatello

ISBN 978-953-307-418-4

Hard cover, 490 pages

**Publisher** InTech

**Published online** 14, November, 2011

**Published in print edition** November, 2011

These contribution books collect reviews and original articles from eminent experts working in the interdisciplinary arena of biomaterial development and use. From their direct and recent experience, the readers can achieve a wide vision on the new and ongoing potentialities of different synthetic and engineered biomaterials. Contributions were selected not based on a direct market or clinical interest, but based on results coming from very fundamental studies. This too will allow to gain a more general view of what and how the various biomaterials can do and work for, along with the methodologies necessary to design, develop and characterize them, without the restrictions necessarily imposed by industrial or profit concerns. The chapters have been arranged to give readers an organized view of this research area. In particular, this book contains 25 chapters related to recent researches on new and known materials, with a particular attention to their physical, mechanical and chemical characterization, along with biocompatibility and histopathological studies. Readers will be guided inside the range of disciplines and design methodologies used to develop biomaterials possessing the physical and biological properties needed for specific medical and clinical applications.

### **How to reference**

In order to correctly reference this scholarly work, feel free to copy and paste the following:

Foued Ben Ayed (2011). Elaboration and Characterization of Calcium Phosphate Biomaterial for Biomedical Applications, Biomaterials - Physics and Chemistry, Prof. Rosario Pignatello (Ed.), ISBN: 978-953-307-418-4, InTech, Available from: <http://www.intechopen.com/books/biomaterials-physics-and-chemistry/elaboration-and-characterization-of-calcium-phosphate-biomaterial-for-biomedical-applications>

**INTECH**  
open science | open minds

#### **InTech Europe**

University Campus STeP Ri  
Slavka Krautzeka 83/A  
51000 Rijeka, Croatia  
Phone: +385 (51) 770 447  
Fax: +385 (51) 686 166  
[www.intechopen.com](http://www.intechopen.com)

#### **InTech China**

Unit 405, Office Block, Hotel Equatorial Shanghai  
No.65, Yan An Road (West), Shanghai, 200040, China  
中国上海市延安西路65号上海国际贵都大饭店办公楼405单元  
Phone: +86-21-62489820  
Fax: +86-21-62489821

© 2011 The Author(s). Licensee IntechOpen. This is an open access article distributed under the terms of the [Creative Commons Attribution 3.0 License](#), which permits unrestricted use, distribution, and reproduction in any medium, provided the original work is properly cited.

IntechOpen

IntechOpen